

Single-Coupling Bounds on R-parity violating Supersymmetry, an update

Yee Kao* and Tatsu Takeuchi†

*Institute for Particle, Nuclear, and Astronomical Sciences,
Physics Department, Virginia Tech, Blacksburg, VA 24061*

We update the single-coupling bounds on R-parity violating supersymmetry using the most up to date data as of October 2009. In addition to the data listed in the 2009 Review of Particle Properties [1], we utilize a new determination of the weak charge of cesium-133 [2], and preliminary τ -decay branching fractions from Babar [3]. Analysis of semileptonic D -decay is improved by the inclusion of experimentally measured form-factors into the calculation of the Standard Model predictions.

PACS numbers: 11.30.Hv, 12.60.Jv, 13.20.-v, 14.60.-z

I. INTRODUCTION

R-parity violating supersymmetry (SUSY) interactions [4, 5] provide a convenient framework for quantifying quark- and lepton-flavor violating effects that new physics beyond the Standard Model (SM) may have, independently of whether SUSY truly exists in nature or not. Consequently, various authors have used a variety of flavor sensitive observables to constrain the sizes of these couplings [5, 6, 7, 8, 9, 10, 11, 12, 13, 14, 15, 16]. In this paper, we update the single-coupling bounds, namely the bounds on the individual R-parity violating couplings when only that particular coupling is assumed to be non-zero, using the most up to date precision data available as of October 2009. These include various lepton and meson decay ratios, CKM matrix elements, and the weak charge of atomic nuclei.

The superpotential of R-parity violating SUSY interactions is given by [4, 5]

$$W_{\mathcal{R}} = \frac{1}{2} \lambda_{ijk} \hat{L}_i \hat{L}_j \hat{E}_k + \lambda'_{ijk} \hat{L}_i \hat{Q}_j \hat{D}_k + \frac{1}{2} \lambda''_{ijk} \hat{U}_i \hat{D}_j \hat{D}_k. \quad (1)$$

Here i, j, k are generation indices, while $SU(2)$ -weak isospin and $SU(3)$ -color indices are suppressed. The coefficients λ_{ijk} are antisymmetric in the first two indices, while λ''_{ijk} are antisymmetric in the latter two. Consequently, there are 9 independent LLE couplings, 27 independent LQD couplings, and 9 independent UDD couplings. The λ''_{ijk} couplings lead to baryon number violating effects and are already very strongly constrained by proton decay [5], either individually [17] or in products with the λ_{ijk} and λ'_{ijk} couplings [18], so they will not be considered here.

The explicit forms of the LLE and LQD interactions in terms of four-component spinors are

$$\begin{aligned} \mathcal{L}_{LLE} &= \lambda_{(i<j)k} \left[\left(\tilde{\nu}_{iL} \bar{e}_{kR} e_{jL} + \tilde{e}_{jL} \bar{e}_{kR} \nu_{iL} + \tilde{e}_{kR}^* \bar{\nu}_{iL}^c e_{jL} \right) - \left(\tilde{\nu}_{jL} \bar{e}_{kR} e_{iL} + \tilde{e}_{iL} \bar{e}_{kR} \nu_{jL} + \tilde{e}_{kR}^* \bar{\nu}_{jL}^c e_{iL} \right) \right] + h.c. \\ \mathcal{L}_{LQD} &= \lambda'_{ijk} \left[\left(\tilde{\nu}_{iL} \bar{d}_{kR} d_{jL} + \tilde{d}_{jL} \bar{d}_{kR} \nu_{iL} + \tilde{d}_{kR}^* \bar{\nu}_{iL}^c d_{jL} \right) - \left(\tilde{e}_{iL} \bar{d}_{kR} u_{jL} + \tilde{u}_{jL} \bar{d}_{kR} e_{iL} + \tilde{d}_{kR}^* \bar{e}_{iL}^c u_{jL} \right) \right] + h.c. \end{aligned} \quad (2)$$

Note that the charge-conjugated chiral fermion fields are denoted $f_{L/R}^c = (f_{L/R})^c = (f^c)_{R/L}$. The exchange of squarks or sleptons mediate interactions among the SM fermions, and the strength of these interactions will be proportional to the ratio of coupling constant squared to the exchanged sparticle mass squared. To simplify notation, we follow Ref. [5] and define

$$r_{ijk}(\tilde{\ell}) \equiv \frac{1}{4\sqrt{2}G_F} \frac{|\lambda_{ijk}|^2}{M_{\tilde{\ell}}^2}, \quad r'_{ijk}(\tilde{q}) \equiv \frac{1}{4\sqrt{2}G_F} \frac{|\lambda'_{ijk}|^2}{M_{\tilde{q}}^2}. \quad (3)$$

Shifts in various observables will be expressed in terms of these dimensionless parameter combinations. The final bounds on the coupling constant will be shown with all the sparticle masses set to 100 GeV.

*Electronic address: ykao@vt.edu

†Electronic address: takeuchi@vt.edu

In the following sections, we look at the bounds from μ and τ leptonic decays, $\tau \rightarrow \pi\nu$ and π decays, CKM unitarity, semi-leptonic D and leptonic D_s decays, and the weak charge of cesium-133. For analyses involving τ -decay, the impact of preliminary τ -decay data from Babar [3] is discussed. The analysis of semi-leptonic D decay is improved by a new calculation of the Standard Model (SM) predictions which include the effects of experimentally determined form-factors. The analysis of the weak charge of cesium-133 corrects an error in Ref. [5]. Bounds from Z -peak observables are not updated since no new data have been generated since the 2005 review by Barbier et al. [5]. The bound from neutrinoless double beta decay [6] will be discussed in a separate paper [41].

II. μ AND τ DECAY

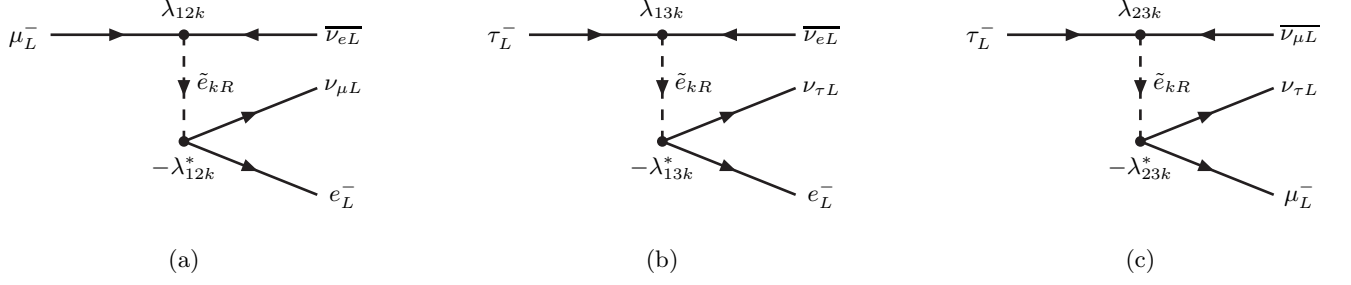


FIG. 1: Possible R-parity violating contributions to (a) $\mu^- \rightarrow e^- \bar{\nu}_e \nu_\mu$, (b) $\tau^- \rightarrow e^- \bar{\nu}_e \nu_\tau$, and (c) $\tau^- \rightarrow \mu^- \bar{\nu}_\mu \nu_\tau$.

The LLE couplings λ_{ijk} affect the decays $\mu^- \rightarrow e^- \bar{\nu}_e \nu_\mu$, $\tau^- \rightarrow e^- \bar{\nu}_e \nu_\tau$, and $\tau^- \rightarrow \mu^- \bar{\nu}_\mu \nu_\tau$. via the processes shown in Fig. 1. The operator induced by the exchange of \tilde{e}_{kR} ($k = 1, 2, 3$) via the coupling $\lambda_{(i<j)k}$ is

$$-\frac{|\lambda_{(i<j)k}|^2}{M_{\tilde{e}_{kR}}^2} (\bar{\nu}_{iL}^c e_{jL}) (\bar{e}_{iL} \nu_{jL}^c) \xrightarrow{\text{Fierz}} -\frac{|\lambda_{(i<j)k}|^2}{2M_{\tilde{e}_{kR}}^2} (\bar{\nu}_{jL} \gamma^\mu e_{jL}) (\bar{e}_{iL} \gamma_\mu \nu_{iL}). \quad (4)$$

This will interfere with the SM operator

$$-\frac{4G_F}{\sqrt{2}} (\bar{\nu}_{jL} \gamma^\mu e_{jL}) (\bar{e}_{iL} \gamma_\mu \nu_{iL}), \quad (i < j), \quad (5)$$

shifting the effective coupling to

$$\frac{4G_F}{\sqrt{2}} \rightarrow \frac{4G_F}{\sqrt{2}} \left[1 + r_{(i<j)k}(\tilde{e}_{kR}) \right]. \quad (6)$$

In particular, λ_{12k} will shift the muon decay constant G_μ to

$$G_\mu \rightarrow G_F \left[1 + r_{12k}(\tilde{e}_{kR}) \right], \quad (7)$$

and this shift will also affect other observables to be discussed later. The ratios

$$R_{\tau\mu} = \frac{\Gamma(\tau^- \rightarrow \mu^- \bar{\nu}_\mu \nu_\tau)}{\Gamma(\mu^- \rightarrow e^- \bar{\nu}_e \nu_\mu)} \quad \text{and} \quad R_\tau = \frac{\Gamma(\tau^- \rightarrow e^- \bar{\nu}_e \nu_\tau)}{\Gamma(\tau^- \rightarrow \mu^- \bar{\nu}_\mu \nu_\tau)} \quad (8)$$

will be shifted to

$$\begin{aligned} R_{\tau\mu} &= [R_{\tau\mu}]_{\text{SM}} \left[1 + 2 \left\{ r_{23k}(\tilde{e}_{kR}) - r_{12k}(\tilde{e}_{kR}) \right\} \right], \\ R_\tau &= [R_\tau]_{\text{SM}} \left[1 + 2 \left\{ r_{13k}(\tilde{e}_{kR}) - r_{23k}(\tilde{e}_{kR}) \right\} \right]. \end{aligned} \quad (9)$$

The SM predictions for the decay widths including radiative corrections [19, 20] are:

$$\Gamma(\tau \rightarrow \mu \bar{\nu}_\mu \nu_\tau (\gamma))_{\text{SM}} = \frac{g^4}{64M_W^4} \frac{m_\tau^5}{96\pi^3} f\left(\frac{m_\mu^2}{m_\tau^2}\right) \delta_W^\tau \delta_\gamma^\tau,$$

	phase space	W propagator	photon
$\Gamma(\tau \rightarrow \mu \bar{\nu}_\mu \nu_\tau)$	$f(m_\mu^2/m_\tau^2) = 0.9726$	$\delta_W^\tau = 1.0003$	$\delta_\gamma^\tau = 0.9957$
$\Gamma(\tau \rightarrow e \bar{\nu}_e \nu_\tau)$	$f(m_e^2/m_\tau^2) = 1.0000$		
$\Gamma(\mu \rightarrow e \bar{\nu}_e \nu_\mu)$	$f(m_e^2/m_\mu^2) = 0.9998$	$\delta_W^\mu = 1.0000$	$\delta_\gamma^\mu = 0.9958$

TABLE I: The corrections to the leptonic decay widths of the τ and μ .

$$\begin{aligned} \Gamma(\tau \rightarrow e \bar{\nu}_e \nu_\tau (\gamma))_{\text{SM}} &= \frac{g^4}{64M_W^4} \frac{m_\tau^5}{96\pi^3} f\left(\frac{m_e^2}{m_\tau^2}\right) \delta_W^\tau \delta_\gamma^\tau, \\ \Gamma(\mu \rightarrow e \bar{\nu}_e \nu_\mu (\gamma))_{\text{SM}} &= \frac{g^4}{64M_W^4} \frac{m_\mu^5}{96\pi^3} f\left(\frac{m_e^2}{m_\mu^2}\right) \delta_W^\mu \delta_\gamma^\mu = \frac{1}{\tau_\mu}, \end{aligned} \quad (10)$$

in which $f(x)$ is the phase space factor

$$f(x) = 1 - 8x + 8x^3 - x^4 - 12x^2 \ln x, \quad (11)$$

δ_W^ℓ is the W propagator correction

$$\delta_W^\ell = \left(1 + \frac{3}{5} \frac{m_\ell^2}{M_W^2}\right), \quad (12)$$

δ_γ^ℓ is the radiative correction from photons

$$\delta_\gamma^\ell = 1 + \frac{\alpha(m_\ell)}{2\pi} \left(\frac{25}{4} - \pi^2\right), \quad (13)$$

and the values of the running QED coupling constant at the relevant energies are [20]

$$\begin{aligned} \alpha^{-1}(m_\mu) &= \alpha^{-1} - \frac{2}{3\pi} \ln \frac{m_\mu}{m_e} + \frac{1}{6\pi} \approx 136.0, \\ \alpha^{-1}(m_\tau) &\approx 133.3. \end{aligned} \quad (14)$$

The numerical values of these corrections are shown in Table I. The SM predictions for the ratios are therefore

$$\begin{aligned} [R_{\tau\mu}]_{\text{SM}} &= \frac{\Gamma(\tau \rightarrow \mu \bar{\nu}_\mu \nu_\tau (\gamma))_{\text{SM}}}{\Gamma(\mu \rightarrow e \bar{\nu}_e \nu_\mu (\gamma))_{\text{SM}}} = \frac{m_\tau^5}{m_\mu^5} \frac{f(m_\mu^2/m_\tau^2)}{f(m_e^2/m_\mu^2)} \frac{\delta_W^\tau}{\delta_W^\mu} \frac{\delta_\gamma^\tau}{\delta_\gamma^\mu} = 1.309 \times 10^6, \\ [R_\tau]_{\text{SM}} &= \frac{\Gamma(\tau \rightarrow e \bar{\nu}_e \nu_\tau (\gamma))_{\text{SM}}}{\Gamma(\tau \rightarrow \mu \bar{\nu}_\mu \nu_\tau (\gamma))_{\text{SM}}} = \frac{f(m_e^2/m_\tau^2)}{f(m_\mu^2/m_\tau^2)} = 1.028. \end{aligned} \quad (15)$$

The experimental values of these ratios from the Review of Particle Properties [1] are

$$\begin{aligned} R_{\tau\mu} &= \frac{\tau_\mu}{\tau_\tau} \mathcal{B}(\tau \rightarrow \mu \bar{\nu}_\mu \nu_\tau (\gamma)) = \frac{(2.197034 \pm 0.000021) \times 10^{-6} \text{ s}}{(290.6 \pm 1.0) \times 10^{-15} \text{ s}} (17.36 \pm 0.05)\% = (1.312 \pm 0.006) \times 10^6, \\ R_\tau &= \frac{\mathcal{B}(\tau \rightarrow e \bar{\nu}_e \nu_\tau (\gamma))}{\mathcal{B}(\tau \rightarrow \mu \bar{\nu}_\mu \nu_\tau (\gamma))} = \frac{(17.85 \pm 0.05)\%}{(17.36 \pm 0.05)\%} = 1.028 \pm 0.004. \end{aligned} \quad (16)$$

The effect of a -13% correlation between $\mathcal{B}(\tau \rightarrow e \bar{\nu}_e \nu_\tau (\gamma))$ and $\mathcal{B}(\tau \rightarrow \mu \bar{\nu}_\mu \nu_\tau (\gamma))$ on the error on R_τ is small. Allowing only one of the λ 's to be non-zero at a time, comparison of Eqs. (9), (15), and (16) places the following 2σ bounds:

$$\begin{aligned} |\lambda_{12k}| \left(\frac{100 \text{ GeV}}{M_{\bar{e}_{kR}}}\right) &< 0.05 [R_{\tau\mu}], \\ |\lambda_{13k}| \left(\frac{100 \text{ GeV}}{M_{\bar{e}_{kR}}}\right) &< 0.05 [R_\tau], \\ |\lambda_{23k}| \left(\frac{100 \text{ GeV}}{M_{\bar{e}_{kR}}}\right) &< 0.05 [R_\tau], 0.06 [R_{\tau\mu}]. \end{aligned} \quad (17)$$

A new but still preliminary value of R_τ from Babar was announced at ICHEP 2008 [3] as

$$[R_\tau]_{\text{Babar2008}} = \frac{1}{0.9796 \pm 0.0038} = 1.021 \pm 0.004. \quad (18)$$

Including this value will change the world average to

$$R_\tau = 1.025 \pm 0.003 ,$$

and the corresponding 2σ bounds will be

$$|\lambda_{13k}| \left(\frac{100 \text{ GeV}}{M_{\tilde{e}_{kR}}} \right) < 0.03 [R_\tau] , \quad |\lambda_{23k}| \left(\frac{100 \text{ GeV}}{M_{\tilde{e}_{kR}}} \right) < 0.05 [R_\tau] . \quad (19)$$

We see that the bound on λ_{13k} will be tightened.

III. π AND τ DECAY

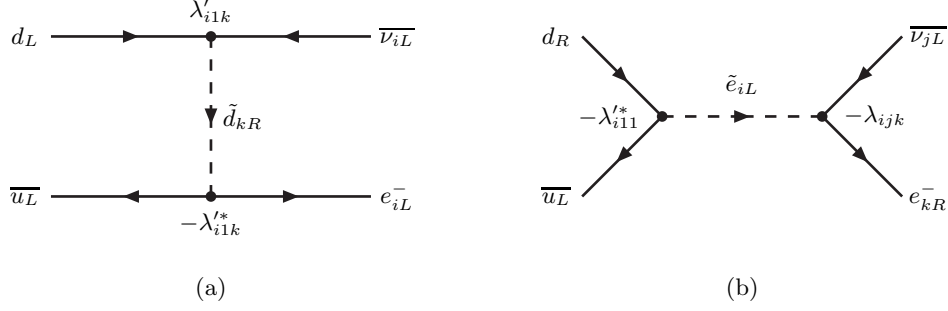


FIG. 2: Possible R-parity violating contributions to $\pi^- \rightarrow \ell^- \bar{\nu}_\ell$ ($\ell = e_1 = e$, or $e_2 = \mu$) that interfere with the SM amplitude. The indices are $i = 1$ or 2 , $k = 1, 2, 3$ in (a); while $(jk) = (11)$ or (22) , with $i = 3 - j$ or 3 in (b) due to the anti-symmetry of λ_{ijk} in the first two indices. The interference of (b) with the SM amplitude is suppressed due to the smallness of the electron mass.

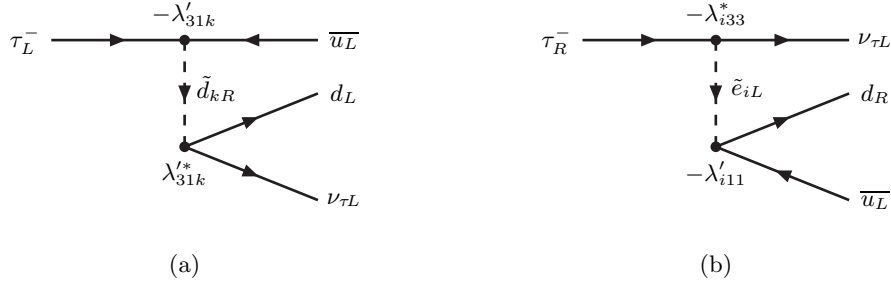


FIG. 3: Possible R-parity violating contributions to the decay $\tau^- \rightarrow \pi^- \nu_\tau$.

Possible R-parity violating contributions to the decay $\pi^- \rightarrow \ell^- \bar{\nu}_\ell$ ($\ell = e$ or μ) are shown in Fig. 2, and those to $\tau^- \rightarrow \pi^- \nu_\tau$ are shown in Fig. 3. Since we are only interested in placing bounds on the individual R-parity violating couplings separately, we will ignore the (b) diagrams in both cases.

The processes of Fig. 2(a) and Fig. 3(a) induce the following operators:

$$\begin{aligned} 2(a) : & \quad -\frac{|\lambda'_{i1k}|^2}{M_{\tilde{d}_{kR}}^2} (\bar{\nu}_{iL}^c d_{jL}) (\bar{u}_L e_{iL}^c) \xrightarrow{\text{Fierz}} -\frac{|\lambda_{i1k}|^2}{2M_{\tilde{d}_{kR}}^2} (\bar{\nu}_{iL}^c \gamma^\mu e_{iL}^c) (\bar{u}_L \gamma_\mu d_L) = -\frac{|\lambda_{i1k}|^2}{2M_{\tilde{d}_{kR}}^2} (\bar{e}_{iL} \gamma^\mu \nu_{iL}) (\bar{u}_L \gamma_\mu d_L) , \\ 3(a) : & \quad -\frac{|\lambda'_{31k}|^2}{M_{\tilde{d}_{kR}}^2} (\bar{\tau}_L^c u_L) (\bar{d}_L \nu_{\tau L}^c) \xrightarrow{\text{Fierz}} -\frac{|\lambda_{31k}|^2}{2M_{\tilde{d}_{kR}}^2} (\bar{\tau}_L^c \gamma^\mu \nu_{\tau L}^c) (\bar{d}_L \gamma_\mu u_L) = -\frac{|\lambda_{31k}|^2}{2M_{\tilde{d}_{kR}}^2} (\bar{\nu}_{\tau L} \gamma^\mu \tau_L) (\bar{d}_L \gamma_\mu u_L) . \end{aligned} \quad (20)$$

These interfere with the SM operators given by

$$-\frac{4G_F}{\sqrt{2}} V_{ud} (\bar{e}_{iL} \gamma^\mu \nu_{iL}) (\bar{u}_L \gamma_\mu d_L) , \quad \text{and} \quad -\frac{4G_F}{\sqrt{2}} V_{ud}^* (\bar{\nu}_{\tau L} \gamma^\mu \tau_L) (\bar{d}_L \gamma_\mu u_L) , \quad (21)$$

and shift the π -decay widths to

$$\Gamma(\pi^- \rightarrow \ell_i^- \bar{\nu}_{\ell_i}) = [\Gamma(\pi^- \rightarrow \ell_i^- \bar{\nu}_{\ell_i})]_{\text{SM}} \left[1 + \frac{2}{|V_{ud}|} r'_{i1k}(\tilde{d}_{kR}) \right], \quad (22)$$

while the τ -decay width is shifted by

$$\Gamma(\tau^- \rightarrow \pi^- \nu_\tau) = [\Gamma(\tau^- \rightarrow \pi^- \nu_\tau)]_{\text{SM}} \left[1 + \frac{2}{|V_{ud}|} r'_{31k}(\tilde{d}_{kR}) \right]. \quad (23)$$

Here, we have neglected any relative phase between the SM and RPV contributions. The ratios

$$\begin{aligned} R_\pi &= \frac{\Gamma(\pi^- \rightarrow e^- \bar{\nu}_e)}{\Gamma(\pi^- \rightarrow \mu^- \bar{\nu}_\mu)}, \\ R_{\tau\pi} &= \frac{\Gamma(\tau^- \rightarrow \pi^- \nu_\tau)}{\Gamma(\pi^- \rightarrow \mu^- \bar{\nu}_\mu)}, \end{aligned} \quad (24)$$

are shifted to

$$\begin{aligned} R_\pi &= [R_\pi]_{\text{SM}} \left[1 + \frac{2}{|V_{ud}|} \left\{ r'_{11k}(\tilde{d}_{kR}) - r'_{21k}(\tilde{d}_{kR}) \right\} \right], \\ R_{\tau\pi} &= [R_{\tau\pi}]_{\text{SM}} \left[1 + \frac{2}{|V_{ud}|} \left\{ r'_{21k}(\tilde{d}_{kR}) - r'_{31k}(\tilde{d}_{kR}) \right\} \right]. \end{aligned} \quad (25)$$

At tree level, the SM prediction for the π -decay widths is given by

$$[\Gamma(\pi^- \rightarrow \ell^- \bar{\nu}_\ell)]_{\text{SM,tree}} = \left(\sqrt{2} G_F |V_{ud}| \right)^2 \frac{m_\ell^2 m_\pi}{16\pi} \left(1 - \frac{m_\ell^2}{m_\pi^2} \right)^2 f_\pi^2, \quad (26)$$

while that of τ -decay into $\pi \nu_\tau$ is

$$[\Gamma(\tau^- \rightarrow \pi^- \nu_\tau)]_{\text{SM,tree}} = \left(\sqrt{2} G_F |V_{ud}| \right)^2 \frac{m_\tau^3}{32\pi} \left(1 - \frac{m_\pi^2}{m_\tau^2} \right)^2 f_\pi^2, \quad (27)$$

where the pion decay constant f_π is normalized as

$$\langle 0 | \bar{u} \gamma_\mu \gamma_5 d(0) | \pi^-(\mathbf{q}) \rangle = i q_\mu f_\pi. \quad (28)$$

Taking ratios, we find

$$\begin{aligned} [R_\pi]_{\text{SM,tree}} &= \frac{[\Gamma(\pi^- \rightarrow e^- \bar{\nu}_e)]_{\text{SM,tree}}}{[\Gamma(\pi^- \rightarrow \mu^- \bar{\nu}_\mu)]_{\text{SM,tree}}} = \frac{m_e^2 (1 - m_e^2/m_\pi^2)^2}{m_\mu^2 (1 - m_\mu^2/m_\pi^2)^2} = 1.283 \times 10^{-4}, \\ [R_{\tau\pi}]_{\text{SM,tree}} &= \frac{[\Gamma(\tau^- \rightarrow \pi^- \nu_\tau)]_{\text{SM,tree}}}{[\Gamma(\pi^- \rightarrow \mu^- \bar{\nu}_\mu)]_{\text{SM,tree}}} = \frac{m_\tau^3 (1 - m_\pi^2/m_\tau^2)^2}{2m_\mu^2 m_\pi (1 - m_\mu^2/m_\pi^2)^2} = 9.756 \times 10^3. \end{aligned} \quad (29)$$

Radiative corrections to these relations have been calculated in Ref. [21] and modify them to

$$\begin{aligned} [R_\pi]_{\text{SM}} &= [R_\pi]_{\text{SM,tree}} (1 + \delta R_\pi), \\ [R_{\tau\pi}]_{\text{SM}} &= [R_{\tau\pi}]_{\text{SM,tree}} (1 + \delta R_{\tau\pi}), \end{aligned} \quad (30)$$

with

$$\delta R_\pi = -0.0374 \pm 0.0001, \quad \delta R_{\tau\pi} = +0.0016_{-0.0014}^{+0.0009}. \quad (31)$$

The uncertainty in these corrections is due to the uncertainty from strong interaction effects. Therefore,

$$\begin{aligned} [R_\pi]_{\text{SM}} &= 1.235 \times 10^{-4}, \\ [R_{\tau\pi}]_{\text{SM}} &= 9.771_{-0.013}^{+0.009} \times 10^3. \end{aligned} \quad (32)$$

On the other hand, the current experimental values are [1]

$$R_\pi = \frac{\mathcal{B}(\pi \rightarrow e \bar{\nu}_e(\gamma))}{\mathcal{B}(\pi \rightarrow \mu \bar{\nu}_\mu(\gamma))} = \frac{(0.01230 \pm 0.00004)\%}{(99.98770 \pm 0.00004)\%} = (1.230 \pm 0.004) \times 10^{-4},$$

$$R_{\tau\pi} = \frac{\tau_\pi}{\tau_\tau} \frac{\mathcal{B}(\tau \rightarrow \pi \nu_\tau (\gamma))}{\mathcal{B}(\pi \rightarrow \mu \bar{\nu}_\mu (\gamma))} = \frac{(2.6033 \pm 0.0005) \times 10^{-8} \text{s}}{(290.6 \pm 1.0) \times 10^{-15} \text{s}} \frac{(10.91 \pm 0.07)\%}{(99.98770 \pm 0.00004)\%} = (9.775 \pm 0.071) \times 10^3. \quad (33)$$

The magnitude of the CKM matrix element V_{ud} is [22],

$$|V_{ud}| = 0.97418 \pm 0.00027. \quad (34)$$

Comparison of Eqs. (25), (32) and (33) leads to the following 2σ bounds assuming only one of the couplings is non-zero at a time:

$$\begin{aligned} |\lambda'_{11k}| \left(\frac{100 \text{ GeV}}{M_{\tilde{d}_{kR}}} \right) &< 0.03 [R_\pi], \\ |\lambda'_{21k}| \left(\frac{100 \text{ GeV}}{M_{\tilde{d}_{kR}}} \right) &< 0.06 [R_\pi], 0.07 [R_{\tau\pi}], \\ |\lambda'_{31k}| \left(\frac{100 \text{ GeV}}{M_{\tilde{d}_{kR}}} \right) &< 0.06 [R_{\tau\pi}]. \end{aligned} \quad (35)$$

Another preliminary result announced at ICHEP 2008 from Babar [3] was

$$\left[\frac{\mathcal{B}(\tau^- \rightarrow \pi^- \nu_\tau)}{\mathcal{B}(\tau^- \rightarrow e^- \bar{\nu}_e \nu_\tau)} \right]_{\text{Babar2008}} = 0.5945 \pm 0.0063. \quad (36)$$

Using the current world average value of $\mathcal{B}(\tau^- \rightarrow e^- \bar{\nu}_e \nu_\tau) = (17.85 \pm 0.05)\%$ [1] we find

$$[\mathcal{B}(\tau^- \rightarrow \pi^- \nu_\tau)]_{\text{Babar2008}} = 10.61 \pm 0.12. \quad (37)$$

Including this value will shift the world average to

$$\mathcal{B}(\tau^- \rightarrow \pi^- \nu_\tau) = 10.83 \pm 0.06, \quad (38)$$

and the ratio $R_{\tau\pi}$ to

$$R_{\tau\pi} = (9.703 \pm 0.063) \times 10^3. \quad (39)$$

The error will be reduced somewhat and the central value shifted down by about 1σ . The 2σ bounds will become

$$|\lambda'_{21k}| \left(\frac{100 \text{ GeV}}{M_{\tilde{d}_{kR}}} \right) < 0.04 [R_{\tau\pi}], \quad |\lambda'_{31k}| \left(\frac{100 \text{ GeV}}{M_{\tilde{d}_{kR}}} \right) < 0.08 [R_{\tau\pi}], \quad (40)$$

the change mostly due to the shift in the central value of $R_{\tau\pi}$.

IV. CKM UNITARITY

The SM values of the CKM matrix elements V_{ud} , V_{us} , and V_{ub} must satisfy the unitarity relation

$$|V_{ud}^{\text{SM}}|^2 + |V_{us}^{\text{SM}}|^2 + |V_{ub}^{\text{SM}}|^2 = 1. \quad (41)$$

Deviation of the measured values from this relation could be a sign of new physics. The value of $|V_{ud}|$, cited above in Eq. (34), is obtained from the comparison of superallowed $0^+ \rightarrow 0^+$ nuclear beta decays and muon decay [22], the former used to extract the product $G_F V_{ud}$ and the latter used to cancel the G_F . The SM operators relevant for these decays are

$$-\frac{4G_F}{\sqrt{2}} V_{ud}^{\text{SM}} (\bar{u}_L \gamma^\mu d_L) (\bar{e}_L \gamma_\mu \nu_{eL}), \quad \text{and} \quad -\frac{4G_F}{\sqrt{2}} (\bar{\nu}_{\mu L} \gamma^\mu \mu_L) (\bar{e}_L \gamma_\mu \nu_{eL}). \quad (42)$$

Any new physics amplitude which interferes with these operators will affect the extracted value of V_{ud} . The first operator is the same as the operator responsible for the decay $\pi^- \rightarrow e^- \bar{\nu}_e$. The RPV amplitudes which interfere with

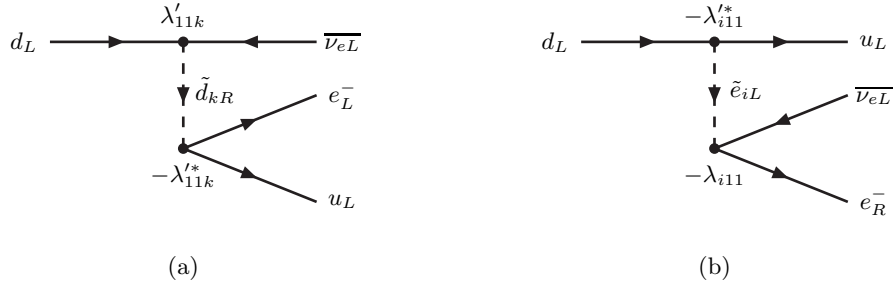
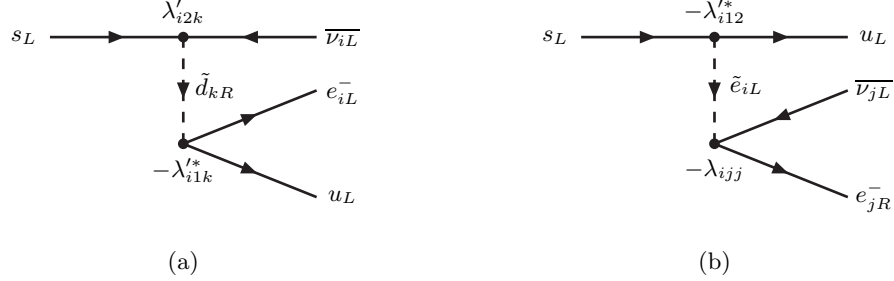


FIG. 4: Possible R-parity violating contributions to nuclear beta decay.

FIG. 5: Possible R-parity violating contributions to semileptonic K -decay.

this are the same as those shown in Fig. 2 except with the u_L lines pointing toward the future as shown in Fig. 4. Since Fig. 4(b) depends on two different RPV couplings (its interference is also suppressed by the electron mass) we will only consider Fig. 4(a) for which the corresponding operator is

$$-\frac{|\lambda'_{11k}|^2}{M_{\tilde{d}_{kR}}^2} (\overline{u_L} e_L^c) (\overline{\nu_{eL}} d_L) \xrightarrow{\text{Fierz}} +\frac{|\lambda'_{11k}|^2}{2M_{\tilde{d}_{kR}}^2} (\overline{u_L} \gamma^\mu d_L) (\overline{\nu_{eL}}^c \gamma_\mu e_L^c) = -\frac{|\lambda'_{11k}|^2}{2M_{\tilde{d}_{kR}}^2} (\overline{u_L} \gamma^\mu d_L) (\overline{e_L} \gamma_\mu \nu_{eL}). \quad (43)$$

We have already discussed muon decay in section II where we found that G_F will be shifted by $r_{12k}(\tilde{e}_{kR})$, *cf.* Eq. (7). Therefore, the shift in V_{ud} will be

$$|V_{ud}|^2 = |V_{ud}^{\text{SM}}|^2 \left[1 + \frac{2}{|V_{ud}|} r'_{11k}(\tilde{d}_{kR}) - 2r_{12k}(\tilde{e}_{kR}) \right]. \quad (44)$$

The values of V_{us} and V_{ub} extracted from semi-leptonic K and B decays are [22, 23]

$$\begin{aligned} |V_{us}| &= 0.2255 \pm 0.0019, \\ |V_{ub}| &= (3.95 \pm 0.35) \times 10^{-3}. \end{aligned} \quad (45)$$

The RPV diagrams that contribute to semi-leptonic K -decay are shown in Fig. 5. Similar diagrams contribute to semi-leptonic B -decay. None of these diagrams depend on a single RPV coupling so we may neglect them and assume

$$V_{us} = V_{us}^{\text{SM}}, \quad V_{ub} = V_{ub}^{\text{SM}}. \quad (46)$$

Then,

$$\left[1 + \frac{2}{|V_{ud}|} r'_{11k}(\tilde{d}_{kR}) - 2r_{12k}(\tilde{e}_{kR}) \right] = \frac{|V_{ud}|^2}{1 - |V_{us}|^2 - |V_{ub}|^2} = 0.9999 \pm 0.0011. \quad (47)$$

The 2σ bounds on the couplings are

$$|\lambda'_{11k}| \left(\frac{100 \text{ GeV}}{M_{\tilde{d}_{kR}}} \right) < 0.03 [V_{ud}], \quad |\lambda_{12k}| \left(\frac{100 \text{ GeV}}{M_{\tilde{e}_{kR}}} \right) < 0.03 [V_{ud}]. \quad (48)$$

V. SEMI-LEPTONIC D AND LEPTONIC D_s -DECAY

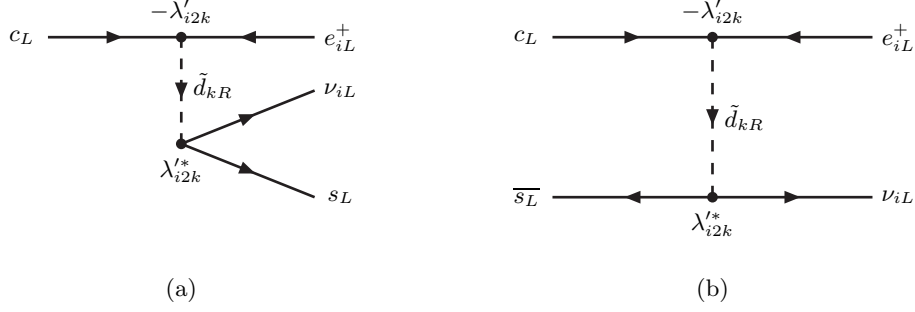


FIG. 6: Possible R-parity violating contributions to semileptonic D -decay and leptonic D_s -decay.

The process shown in Fig. 6(a) affects semileptonic D -decay, while that in Fig. 6(b) affects leptonic D_s -decay. They are both described by the same operator given by

$$-\frac{|\lambda'_{i2k}|^2}{M_{\tilde{d}_{kR}}^2} (\overline{e_{iL}^c} c_L) (\overline{s_L} \nu_{iL}^c) \xrightarrow{\text{Fierz}} -\frac{|\lambda_{i2k}|^2}{2M_{\tilde{d}_{kR}}^2} (\overline{e_{iL}^c} \gamma^\mu \nu_{iL}^c) (\overline{s_L} \gamma_\mu c_L) = -\frac{|\lambda_{i2k}|^2}{2M_{\tilde{d}_{kR}}^2} (\overline{\nu_{iL}} \gamma^\mu e_{iL}) (\overline{s_L} \gamma_\mu c_L). \quad (49)$$

This interferes with the SM operator

$$-\frac{4G_F}{\sqrt{2}} V_{cs}^* (\overline{\nu_{iL}} \gamma^\mu e_{iL}) (\overline{s_L} \gamma_\mu c_L), \quad (50)$$

shifting the D and D_s decay widths by

$$\frac{\Gamma(D \rightarrow K \ell_i \nu_{\ell_i})}{[\Gamma(D \rightarrow K \ell_i \nu_{\ell_i})]_{\text{SM}}} = \frac{\Gamma(D \rightarrow K^* \ell_i \nu_{\ell_i})}{[\Gamma(D \rightarrow K^* \ell_i \nu_{\ell_i})]_{\text{SM}}} = \frac{\Gamma(D_s \rightarrow \ell_i \nu_{\ell_i})}{[\Gamma(D_s \rightarrow \ell_i \nu_{\ell_i})]_{\text{SM}}} = 1 + \frac{2}{|V_{cs}|} r'_{i2k}(\tilde{d}_{kR}), \quad (51)$$

where we have neglected any relative phase between the SM and RPV contributions. Following Ref. [5], we define the ratios

$$\begin{aligned} R_{D^0} &= \frac{\mathcal{B}(D^0 \rightarrow \mu^+ \nu_\mu K^-)}{\mathcal{B}(D^0 \rightarrow e^+ \nu_e K^-)}, \\ R_{D^+} &= \frac{\mathcal{B}(D^+ \rightarrow \mu^+ \nu_\mu \overline{K^0})}{\mathcal{B}(D^+ \rightarrow e^+ \nu_e \overline{K^0})}, \\ R_{D^+}^* &= \frac{\mathcal{B}(D^+ \rightarrow \mu^+ \nu_\mu \overline{K^*(892)^0})}{\mathcal{B}(D^+ \rightarrow e^+ \nu_e \overline{K^*(892)^0})}, \end{aligned} \quad (52)$$

the shifts of which are

$$\frac{R_{D^0}}{[R_{D^0}]_{\text{SM}}} = \frac{R_{D^+}}{[R_{D^+}]_{\text{SM}}} = \frac{R_{D^+}^*}{[R_{D^+}^*]_{\text{SM}}} = 1 + \frac{2}{|V_{cs}|} \left\{ r'_{22k}(\tilde{d}_{kR}) - r'_{12k}(\tilde{d}_{kR}) \right\}. \quad (53)$$

The experimental values of these ratios are currently [1]

$$\begin{aligned} R_{D^0} &= \frac{(3.32 \pm 0.13) \times 10^{-2}}{(3.61 \pm 0.05) \times 10^{-2}} = 0.92 \pm 0.04, \\ R_{D^+} &= \frac{(9.4 \pm 0.8) \times 10^{-2}}{(8.50 \pm 0.26) \times 10^{-2}} = 1.1 \pm 0.1, \\ R_{D^+}^* &= \frac{(5.4 \pm 0.5) \times 10^{-2}}{(5.51 \pm 0.31) \times 10^{-2}} = 0.98 \pm 0.10. \end{aligned} \quad (54)$$

Calculating the SM predictions of these ratios requires knowledge of the form-factors for the matrix elements [24]

$$\langle K | \overline{s} \gamma^\mu (1 - \gamma_5) c | D \rangle \quad \text{and} \quad \langle K^* | \overline{s} \gamma^\mu (1 - \gamma_5) c | D \rangle, \quad (55)$$

for which good experimental data now exist from FOCUS [25, 26, 27], Belle [28], Babar [29], and CLEO [30, 31]. Details of our calculation are presented in the appendix. The results are:

$$\begin{aligned} [R_{D^0}]_{\text{SM}}^{-1} &= [R_{D^+}]_{\text{SM}}^{-1} = 1.04 \pm 0.02 (1\sigma), & 1.04_{-0.06}^{+0.02} (2\sigma), \\ [R_{D^+}^*]_{\text{SM}}^{-1} &= 1.060_{-0.003}^{+0.002} (1\sigma), & 1.060_{-0.007}^{+0.005} (2\sigma). \end{aligned} \quad (56)$$

The analysis of Ref. [5] used the value of $(1.03)^{-1}$ without any errors for all three ratios. This would be the value of R_{D^0} and R_{D^+} if form factors are ignored and the D and the K treated as point particles with the interaction $(K^\dagger \overleftrightarrow{\partial}_\mu D)W^\mu$, and it lies within our calculated range above. For the ratio $R_{D^+}^*$, if form factors are ignored and the D and the K^* treated as point particles with the interaction $K_\mu^{*\dagger} D W^\mu$, its value would be $(1.12)^{-1}$, which illustrates the importance of taking form-factors into account. The value of $|V_{cs}|$, also extracted from D semileptonic decays and D_s leptonic decays [22], is

$$|V_{cs}| = 1.04 \pm 0.06, \quad (57)$$

and for our current purpose we can set it to one. In comparing Eqs. (53), (54), and (56), we allow the SM predictions to scan the entire 2σ range of Eq. (56) and pick up the weakest bounds on the couplings. The resulting 2σ bounds are

$$\begin{aligned} |\lambda'_{12k}| \left(\frac{100 \text{ GeV}}{M_{\tilde{d}_{kR}}} \right) &< 0.2 [R_{D^0}], \quad 0.2 [R_{D^+}], \quad 0.2 [R_{D^+}^*], \\ |\lambda'_{22k}| \left(\frac{100 \text{ GeV}}{M_{\tilde{d}_{kR}}} \right) &< 0.1 [R_{D^0}], \quad 0.4 [R_{D^+}], \quad 0.3 [R_{D^+}^*]. \end{aligned} \quad (58)$$

Next, define

$$R_{D_s}(\tau\mu) = \frac{\mathcal{B}(D_s^+ \rightarrow \tau^+ \nu_\tau)}{\mathcal{B}(D_s^+ \rightarrow \mu^+ \nu_\mu)}. \quad (59)$$

The shift of this ratio is

$$\frac{R_{D_s}(\tau\mu)}{[R_{D_s}(\tau\mu)]_{\text{SM}}} = 1 + \frac{2}{|V_{cs}|} \left\{ r'_{32k}(\tilde{d}_{kR}) - r'_{22k}(\tilde{d}_{kR}) \right\}. \quad (60)$$

The current experimental value is

$$R_{D_s}(\tau\mu) = \frac{(6.6 \pm 0.5) \times 10^{-2}}{(6.3 \pm 0.5) \times 10^{-3}} = 10.5 \pm 1.1, \quad (61)$$

while the tree-level SM prediction is

$$R_{D_s}(\tau\mu) = \frac{m_\tau^2 (1 - m_\tau^2/m_{D_s}^2)^2}{m_\mu^2 (1 - m_\mu^2/m_{D_s}^2)^2} = 9.76 \pm 0.03. \quad (62)$$

Comparison of the two leads to the 2σ bounds given by

$$|\lambda'_{22k}| \left(\frac{100 \text{ GeV}}{M_{\tilde{d}_{kR}}} \right) < 0.2 [R_{D_s}(\tau\mu)], \quad |\lambda'_{32k}| \left(\frac{100 \text{ GeV}}{M_{\tilde{d}_{kR}}} \right) < 0.3 [R_{D_s}(\tau\mu)]. \quad (63)$$

VI. ATOMIC PARITY VIOLATION

The diagrams shown in Fig. (7) lead to the following effective couplings between the quarks and the electron:

$$(a) : \quad \frac{|\lambda'_{11k}|^2}{M_{\tilde{d}_{kR}}^2} (\bar{e}_L^c u_L) (\bar{u}_L e_L^c) \xrightarrow{\text{Fierz}} -\frac{|\lambda'_{11k}|^2}{2M_{\tilde{d}_{kR}}^2} (\bar{e}_L^c \gamma_\mu e_L) (\bar{u}_L \gamma^\mu u_L) = \frac{|\lambda'_{11k}|^2}{2M_{\tilde{d}_{kR}}^2} (\bar{e}_L \gamma_\mu e_L) (\bar{u}_L \gamma^\mu u_L),$$

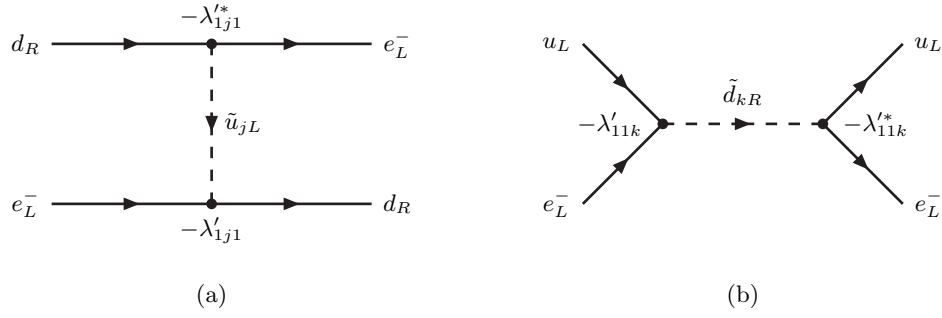


FIG. 7: Possible R-parity violating contributions to atomic parity violation.

$$(b) : \quad \frac{|\lambda'_{1j1}|^2}{M_{\tilde{u}_{jL}}^2} (\bar{e}_L d_R) (\bar{d}_R e_L) \xrightarrow{\text{Fierz}} -\frac{|\lambda'_{1j1}|^2}{2M_{\tilde{u}_{jL}}^2} (\bar{e}_L \gamma^\mu e_L) (\bar{d}_R \gamma_\mu d_R) . \quad (64)$$

The parity violating parts of these interactions are

$$(a) : \quad -\frac{|\lambda'_{11k}|^2}{8M_{\tilde{d}_{kR}}^2} \left[(\bar{e} \gamma_\mu \gamma_5 e) (\bar{u} \gamma^\mu u) + (\bar{e} \gamma_\mu e) (\bar{u} \gamma^\mu \gamma_5 u) \right] ,$$

$$(b) : \quad \frac{|\lambda'_{1j1}|^2}{8M_{\tilde{u}_{jL}}^2} \left[(\bar{e} \gamma_\mu \gamma_5 e) (\bar{d} \gamma^\mu d) - (\bar{e} \gamma_\mu e) (\bar{d} \gamma^\mu \gamma_5 d) \right] . \quad (65)$$

The parity violating SM interactions, on the other hand, are

$$\frac{G_F}{\sqrt{2}} \sum_{q=u,d} \left[C_{1q} (\bar{e} \gamma_\mu \gamma_5 e) (\bar{q} \gamma^\mu q) + C_{2q} (\bar{e} \gamma_\mu e) (\bar{q} \gamma^\mu \gamma_5 q) \right] , \quad (66)$$

with

$$C_{1u} = -\frac{1}{2} + \frac{4}{3}s^2 , \quad C_{2u} = -\frac{1}{2} + 2s^2 ,$$

$$C_{1d} = +\frac{1}{2} - \frac{2}{3}s^2 , \quad C_{2d} = +\frac{1}{2} - 2s^2 , \quad (67)$$

at tree-level, s^2 being the shorthand for $\sin^2 \theta_W$. The weak charge of an atomic nucleus with Z protons and N neutrons is given by

$$Q_W(Z, N) = -2 \left[C_{1u}(2Z + N) + C_{1d}(Z + 2N) \right] = (1 - 4s^2)Z - N . \quad (68)$$

Note that $(2Z + N)$ and $(Z + 2N)$ are respectively the number of up and down quarks in the nucleus. Since the presence of the above R-parity violating couplings will shift the C_1 couplings to

$$C_{1u} \rightarrow C_{1u} - r'_{11k}(\tilde{d}_{kR}) ,$$

$$C_{1d} \rightarrow C_{1d} + r'_{1j1}(\tilde{u}_{jL}) , \quad (69)$$

the weak charge will be shifted by

$$\delta Q_W(Z, N) = +2 \left[(2Z + N) r'_{11k}(\tilde{d}_{kR}) - (Z + 2N) r'_{1j1}(\tilde{u}_{jL}) \right] . \quad (70)$$

Furthermore, since the quantity that is actually measured in atomic parity violation (APV) experiments is the product $G_F Q_W$, and Q_W is extracted by setting G_F equal to the muon decay constant G_μ , the LLE coupling $r_{12k}(\tilde{e}_{kR})$ can also affect Q_W via Eq. (7):

$$\frac{G_F Q_W}{G_\mu} = Q_W [1 - r_{12k}(\tilde{e}_{kR})] . \quad (71)$$

For cesium-133, the total shift will be

$$\delta Q_W(55, 78) = 376 r'_{11k}(\tilde{d}_{kR}) - 422 r'_{1j1}(\tilde{u}_{jL}) - Q_W(55, 78) r_{12k}(\tilde{e}_{kR}). \quad (72)$$

(This formula differs from that provided on page 82 of Ref. [5] which contains a typo: the factor of -2 on the right-hand-side should not be there. This error seems to have propagated into the bounds listed in Eq. (6.47) on the same page. We correct for this error in quoting the bounds from Ref. [5] in Table II.) The latest experimental value of the weak charge of cesium-133 is [2]

$$Q_W(^{133}\text{Cs}) = -73.16 \pm 0.29 \pm 0.20 = -73.16 \pm 0.35. \quad (73)$$

On the other hand, the SM value provided in the Review of Particle Properties [1] is

$$[Q_W(^{133}\text{Cs})]_{\text{SM}} = -73.16 \pm 0.03, \quad (74)$$

which is based on a global fit to all electroweak observables with radiative corrections only from within the SM. Assuming further radiative corrections from new physics is negligibly small, and saturating the difference between the two with the RPV contributions, we find the following 2σ bounds:

$$\lambda'_{11k} \left(\frac{100 \text{ GeV}}{M_{\tilde{d}_{kR}}} \right) < 0.04 [Q_W], \quad \lambda'_{1j1} \left(\frac{100 \text{ GeV}}{M_{\tilde{u}_{jL}}} \right) < 0.03 [Q_W], \quad \lambda_{12k} \left(\frac{100 \text{ GeV}}{M_{\tilde{e}_{kR}}} \right) < 0.08 [Q_W]. \quad (75)$$

VII. SUMMARY

Coupling	Observable	Previous 2σ bound [5]	New 2σ bound	with Babar preliminary [3]
λ_{12k}	V_{ud}	0.05	0.03	
	$R_{\tau\mu}$	0.07	0.05	
	$Q_W(\text{Cs})$	0.11*	0.08	
λ_{13k}	R_τ	0.07	0.05	0.03
λ_{23k}	R_τ	0.07	0.05	0.05
	$R_{\tau\mu}$	0.07	0.06	
λ'_{1j1}	$Q_W(\text{Cs})$	0.03*	0.03	
λ'_{11k}	V_{ud}	0.02	0.03	
	R_π	0.03	0.03	
	$Q_W(\text{Cs})$	0.05*	0.04	
λ'_{12k}	R_{D^0}	0.27 [†]	0.2	
	R_{D^+}	0.44 [†]	0.2	
	$R_{D^+}^*$	0.23 [†]	0.2	
λ'_{21k}	R_π	0.06	0.06	
	$R_{\tau\pi}$	0.08	0.07	0.04
λ'_{22k}	R_{D^0}	0.21 [†]	0.1	
	R_{D^+}	0.61 [†]	0.4	
	$R_{D^+}^*$	0.38 [†]	0.3	
	$R_{D_s}(\tau\mu)$	0.65	0.2	
λ'_{31k}	$R_{\tau\pi}$	0.12	0.06	0.08
λ'_{32k}	$R_{D_s}(\tau\mu)$	0.52	0.3	

TABLE II: Current single-coupling bounds on various RPV couplings compared with those given in Table 6.1 of Ref. [5]. All particle masses have been set to 100 GeV. The values with an asterisk have been corrected for an error in Ref. [5]. Those with a dagger were calculated with the SM prediction fixed to $(1.03)^{-1}$ without any uncertainties.

In this paper, we have looked at a variety of single-coupling bounds that can be imposed on R-parity violation from particle decay ratios and atomic parity violation. Our results are summarized in Table II. Compared to the bounds compiled in 2004 by Barbier et al. [5], the bounds have steadily improved. For the bounds from observables involving

τ -decay, the improvement is due to the results of ALEPH [32] released in 2005. The bounds from observables involving D and D_s decay have improved due to new data from CLEO [30, 33, 34, 35] and Belle [28, 36]. The new bounds from the weak charge of cesium-133 is due to the reduction of theoretical uncertainty in its extraction from experimental data [2].

Further improvements on the bounds from observables involving τ -decay is expected as analyses of Belle and Babar data get under way, each with hundreds of millions of $\tau^+\tau^-$ pairs, as is evidenced by the effect of the preliminary Babar data from 2008 [3]. The bounds from observables involving π -decay can also be expected to improve considerably in the near future as the PIENU experiment at TRIUMF [37] and the PEN experiment and PSI [38] start their physics runs this year, eventually improving the error on R_π by almost an order of magnitude.

The bound on λ'_{111} from neutrinoless double beta decay will be updated in a subsequent paper [41].

Acknowledgements

This work was supported by the U.S. Department of Energy, grant DE-FG05-92ER40709, Task A.

APPENDIX A: SEMILEPTONIC D DECAY RATIOS WITH FORM-FACTORS

The semileptonic decays $D \rightarrow K\ell\nu$ ($D^+ \rightarrow \bar{K}^0\ell^+\nu_\ell$ or $D^0 \rightarrow K^-\ell^+\nu_\ell$) and $D \rightarrow K^*\ell\nu$ ($D^+ \rightarrow \bar{K}^*(892)^0\ell^+\nu_\ell$ or $D^0 \rightarrow K^*(892)^-\ell^+\nu_\ell$) proceed via the SM interaction

$$\mathcal{L} = -\frac{G_F}{\sqrt{2}}V_{cs}^*[\bar{s}\gamma_\mu(1-\gamma_5)c][\bar{\nu}\gamma^\mu(1-\gamma_5)\ell]. \quad (\text{A1})$$

For both cases, the hadronic matrix element is expressed in terms of multiple form factors. In this appendix, we calculate the ratios R_{D^0} , R_{D^+} , and $R_{D^+}^*$, defined in Eq. (52), taking the latest experimental data on these form factors into account.

1. $D \rightarrow K\ell\nu$

For the decay $D \rightarrow K\ell\nu$, the form factors are defined as [24]

$$\langle K|\bar{s}\gamma_\mu(1-\gamma_5)c|D\rangle = (P_D + P_K)_\mu f_+(t) + (P_D - P_K)_\mu f_-(t), \quad (\text{A2})$$

where $t = (P_D - P_K)^2$. The decay width in terms of these form factors is

$$\Gamma = \frac{G_F^2|V_{cs}|^2m_D^3}{24\pi^3} \int_{m_\ell^2}^{(m_D-m_K)^2} dt \left[\left\{ \frac{\lambda^{1/2}(t, m_D^2, m_K^2)}{2m_D^2} \right\}^3 \left(1 - \frac{m_\ell^2}{t}\right)^2 \left(1 + \frac{m_\ell^2}{2t}\right) |f_+(t)|^2 + \frac{3}{8} \frac{m_\ell^2}{m_D^2} \left\{ \frac{\lambda^{1/2}(t, m_D^2, m_K^2)}{2m_D^2} \right\} \left(1 - \frac{m_\ell^2}{t}\right)^2 \frac{t}{m_D^2} \left(\frac{m_D^2 - m_K^2}{t}\right)^2 |f_0(t)|^2 \right], \quad (\text{A3})$$

where we have defined

$$f_0(t) \equiv f_+(t) + \frac{t}{m_D^2 - m_K^2} f_-(t), \quad (\text{A4})$$

and

$$\lambda(a, b, c) = a^2 + b^2 + c^2 - 2ab - 2bc - 2ca. \quad (\text{A5})$$

Since $m_\ell^2 \ll m_D^2$, the scalar form factor term is completely negligible for the electron, and the vector form factor $|f_+(t)|$ can be extracted from the t -dependence of $d\Gamma/dt$. The result is fit by the single-pole function

$$f_+(t) = \frac{f_+(0)}{1 - t/m_{\text{pole}}^2}, \quad (\text{A6})$$

where $f_+(0)$ and m_{pole} are adjustable parameters. This form is motivated by the vector meson dominance model [39] which prescribes the following expressions for the form factors [40]:

$$\begin{aligned} f_+(t) &= c_V \frac{1}{1 - t/m_V^2}, \\ f_0(t) &= c_V + c_S \frac{t/m_S^2}{1 - t/m_S^2}. \end{aligned} \quad (\text{A7})$$

Here, c_V and c_S are constants, and m_V and m_S are the masses of the lowest lying D_s -mesons with $J^P = 1^-$ and 0^+ , respectively. Another popular form used to fit the $f_+(t)$ data is the so-called modified-pole function

$$f_+(t) = \frac{f_+(0)}{(1 - t/m_{D_s^*}^2)(1 - \alpha t/m_{D_s^*}^2)}, \quad (\text{A8})$$

where $m_{D_s^*} = 2112$ MeV, and $f_+(0)$ and α are adjustable. The fit values of m_{pole} and α from recent experiments are listed in Table III.

Collaboration	Decay Mode	m_{pole} (GeV)	α	$f_-(0)/f_+(0)$	Reference
FOCUS	$D^0 \rightarrow K^- \mu^+ \nu_\mu$	$1.93 \pm 0.05 \pm 0.03$	$0.28 \pm 0.08 \pm 0.07$	$-1.7^{+1.5}_{-1.4} \pm 0.3$	[25] 2005
Belle	$D^0 \rightarrow \bar{K}^- \ell^+ \nu_\ell$ ($\ell = e, \mu$)	$1.82 \pm 0.04 \pm 0.02$	$0.52 \pm 0.08 \pm 0.06$		[28] 2006
Babar	$D^0 \rightarrow K^- e^+ \nu_e$	$1.884 \pm 0.012 \pm 0.016$	$0.377 \pm 0.023 \pm 0.031$		[29] 2007
CLEO	$D^0 \rightarrow K^- e^+ \nu_e, D^+ \rightarrow \bar{K}^0 e^+ \nu_e$	$1.93 \pm 0.02 \pm 0.01$	$0.30 \pm 0.03 \pm 0.01$		[31] 2009

TABLE III: Recent measurements of the $D \rightarrow K$ form factors.

The forms of the single-pole and modified-pole functions for the CLEO [31] central values of m_{pole} and α are shown in Fig. 8. They deviate from each other considerably beyond $t \sim 2 \text{ GeV}^2$, where data points are absent due to phase-space suppression. However, due to this same phase-space suppression, it turns out that the R_D ratios are insensitive to this difference in the shape of $f_+(t)$ in this region of t , so we adopt the single-pole form for our purpose.

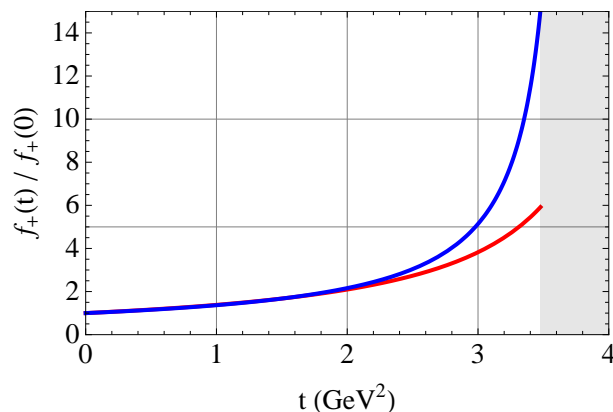


FIG. 8: The single-pole function with $m_{\text{pole}} = 1.93$ GeV (solid), and the modified-pole function with $\alpha = 0.30$ (dashed). The end-point is at $t = m_D^2 \approx 3.5 \text{ GeV}^2$.

FOCUS [25], which looked at the muon channel, has determined the ratio $f_-(0)/f_+(0)$, in addition to m_{pole} and α , by performing a two-dimensional fit to $d^2\Gamma/dt d\cos\theta_\ell$, where θ_ℓ is the angle between the neutrino and the kaon in the $\mu\nu$ rest-frame. If we adopt the meson-dominance form given in Eq. (A7) for $f_0(t)$, with $c_V = f_+(0)$, this ratio determines $r_0 = c_S/c_V$ as

$$r_0 = \frac{c_S}{c_V} = \frac{m_S^2}{m_{\text{pole}}^2} + \frac{m_S^2}{m_D^2 - m_K^2} \frac{f_-(0)}{f_+(0)}. \quad (\text{A9})$$

In the FOCUS analysis, it was assumed that the ratio $f_-(t)/f_+(t)$ was essentially independent of t , which would require $m_S \approx m_{\text{pole}}$. However, as noted above, data points do not extend into the regions of t which are phase-space suppressed, thus m_S can be differ significantly from m_{pole} while still maintaining an almost constant ratio

$f_-(t)/f_+(t)$ in the regions measured. Indeed, in Fig. 9 we show how this ratio varies with t for the two choices $m_S = m_{\text{pole}} = 1930 \text{ MeV}$ and $m_S = m(D_{s0}^*(2317)^\pm) = 2317 \text{ MeV}$ when $f_-(0)/f_+(0) = -1.7$. In the region $t < 2 \text{ GeV}^2$, the ratio only varies from -1.7 to about -1.5 even for the latter case. Thus, in our calculations, we allow m_S to vary between m_{pole} and $m(D_{s0}^*(2317)^\pm)$.

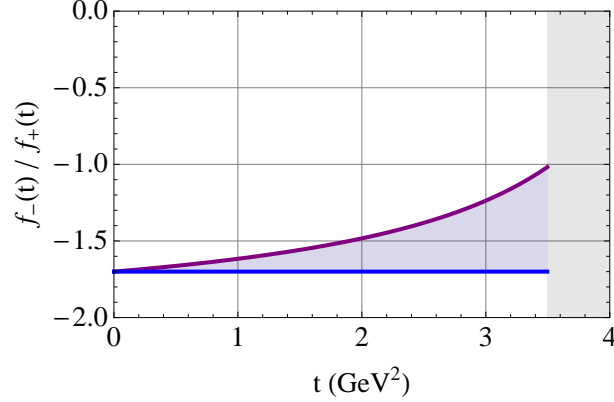


FIG. 9: The ratio $f_-(t)/f_+(t)$ with $m_S = m_{\text{pole}} = 1930 \text{ MeV}$ (solid), and $m_S = m(D_{s0}^*(2317)^\pm) = 2317 \text{ MeV}$ (dashed). The FOCUS central value is used for the value of ratio at $t = 0$.

The form-factors we use are therefore,

$$\begin{aligned} \frac{f_+(t)}{f_+(0)} &= \frac{1}{1 - t/m_{\text{pole}}^2}, \\ \frac{f_0(t)}{f_+(0)} &= 1 + r_0 \frac{t/m_S^2}{1 - t/m_S^2}. \end{aligned} \quad (\text{A10})$$

For m_{pole} we adopt the FOCUS value of 1.93 GeV , which coincides with the CLEO value. The errors on m_{pole} are small enough as to have no effect on R_D since they only change the form of $f_+(t)$ near the pole. The value of r_0 will depend on the value of the ratio $f_-(0)/f_+(0)$ and our choice of m_S as shown in Fig. 10.

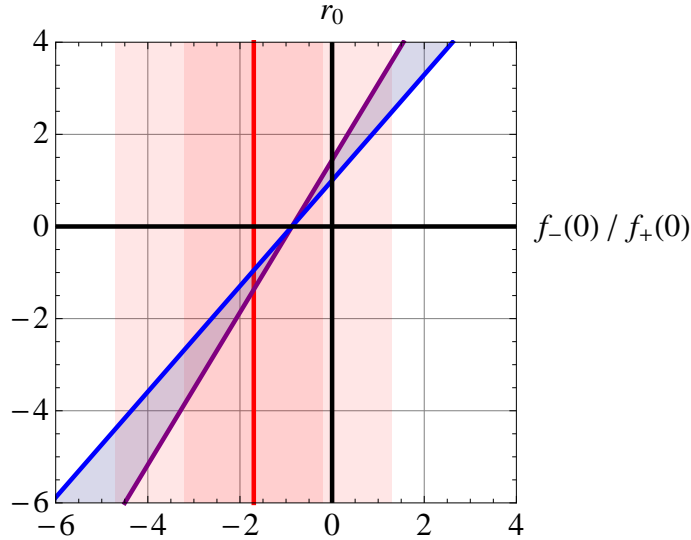


FIG. 10: The dependence of r_0 on the ratio $f_-(0)/f_+(0)$ with $m_S = m_{\text{pole}} = 1930 \text{ MeV}$ (solid), and $m_S = m(D_{s0}^*(2317)^\pm) = 2317 \text{ MeV}$ (dashed). The shaded bands indicate the one- and two-sigma regions of $f_-(0)/f_+(0)$ as measured by FOCUS [25].

Substituting into Eq. (A3), we obtain the values shown in Fig. 11 for $R_D^{-1} = \Gamma(D \rightarrow K e \nu) / \Gamma(D \rightarrow K \mu \nu)$. Reading off from the graph, we assign the following 1σ and 2σ ranges to R_{D^0} and R_{D^+} :

$$(R_{D^0})^{-1} = (R_{D^+})^{-1} = 1.04 \pm 0.02 (1\sigma), \quad 1.04_{-0.06}^{+0.02} (2\sigma). \quad (\text{A11})$$

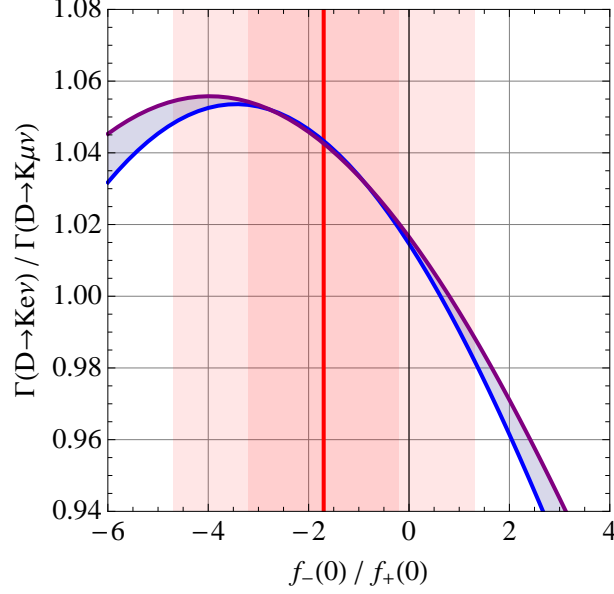


FIG. 11: The dependence of $(R_D)^{-1} = \Gamma(D \rightarrow K^* \ell \nu) / \Gamma(D \rightarrow K \mu \nu)$ on the ratio $f_-(0)/f_+(0)$ with $m_S = m_{\text{pole}} = 1930$ MeV (solid), and $m_S = m(D_{s0}^*(2317)^\pm) = 2317$ MeV (dashed). The shaded bands indicate the one- and two-sigma regions of $f_-(0)/f_+(0)$ as measured by FOCUS [25].

2. $D \rightarrow K^* \ell \nu$

Next, we consider the decay $D \rightarrow K^* \ell \nu_\ell$. The form-factors are defined as [24]

$$\begin{aligned}
& \langle K^*(P_K, \epsilon) | \bar{s} \gamma_\alpha (1 - \gamma_5) c | D(P_D) \rangle \\
&= \varepsilon_{\alpha\beta\gamma\delta} P_D^\beta P_K^\gamma \epsilon^{*\delta} \frac{2}{m_D + m_{K^*}} V(q^2) \\
&+ i \left\{ \epsilon_\alpha^* (m_D + m_{K^*}) A_1(q^2) - \frac{(\epsilon^* \cdot q)}{m_D + m_{K^*}} (P_D + P_K)_\alpha A_2(q^2) - \frac{(\epsilon^* \cdot q)}{q^2} q_\alpha (2m_{K^*}) A_3(q^2) \right\} \\
&+ i \frac{(\epsilon^* \cdot q)}{q^2} q_\alpha (2m_{K^*}) A_0(q^2), \tag{A12}
\end{aligned}$$

where

$$2m_{K^*} A_3(q^2) = (m_D + m_{K^*}) A_1(q^2) - (m_D - m_{K^*}) A_2(q^2), \quad A_3(0) = A_0(0), \tag{A13}$$

and $q^\alpha = (P_D - P_K)^\alpha$. Here, $V(q^2)$ is the contribution of vector intermediate states, while $A_1(q^2)$ and $A_2(q^2)$ are contributions of axial-vector intermediate states. $A_3(q^2)$ combines with $A_1(q^2)$ and $A_2(q^2)$ to maintain the transversality of these axial-vector contributions. $A_0(q^2)$ is the contribution of scalar intermediate states. The condition $A_3(0) = A_0(0)$ is necessary for the cancellation of the poles at $q^2 = 0$. If we rewrite A_3 in terms of A_1 and A_2 , the above expression becomes

$$\begin{aligned}
& \langle K^*(P_K, \epsilon) | \bar{s} \gamma_\alpha (1 - \gamma_5) c | D(P_D) \rangle \\
&= \varepsilon_{\alpha\beta\gamma\delta} P_D^\beta P_K^\gamma \epsilon^{*\delta} \frac{2}{m_D + m_{K^*}} V(q^2) \\
&+ i \left\{ (m_D + m_{K^*}) \left[\epsilon_\alpha^* - \frac{(\epsilon^* \cdot q) q_\alpha}{q^2} \right] A_1(q^2) - \frac{(\epsilon^* \cdot q)}{m_D + m_{K^*}} \left[(P_D + P_K)_\alpha - \frac{(m_D^2 - m_{K^*}^2) q_\alpha}{q^2} \right] A_2(q^2) \right\} \\
&+ i \frac{(\epsilon^* \cdot q)}{q^2} q_\alpha (2m_{K^*}) A_0(q^2), \tag{A14}
\end{aligned}$$

making the transversality of the axial-vector terms manifest. The decay width in terms of these form-factors is

$$\begin{aligned}
\Gamma = & \frac{G_F^2 |V_{cs}|^2 m_D^3}{27 \pi^3} \int_{m_\ell^2}^{(m_D - m_{K^*})^2} dt \\
& \times \left[\frac{4m_D^2}{3(m_D + m_{K^*})^2} \frac{t}{m_D^2} \frac{\lambda^{3/2}(m_D^2, m_{K^*}^2, t)}{m_D^6} \left(1 + \frac{m_\ell^2}{2t}\right) \left(1 - \frac{m_\ell^2}{t}\right)^2 V(t)^2 \right. \\
& + \frac{2(m_D + m_{K^*})^2}{3m_D^2} \frac{t}{m_D^2} \frac{\lambda^{1/2}(m_D^2, m_{K^*}^2, t)}{m_D^2} \left[3 + \frac{\lambda(m_D^2, m_{K^*}^2, t)}{4m_{K^*}^2 t} \right] \left(1 + \frac{m_\ell^2}{2t}\right) \left(1 - \frac{m_\ell^2}{t}\right)^2 A_1(t)^2 \\
& - \frac{(m_D^2 - m_{K^*}^2 - t)}{3m_{K^*}^2} \frac{\lambda^{3/2}(m_D^2, m_{K^*}^2, t)}{m_D^6} \left(1 + \frac{m_\ell^2}{2t}\right) \left(1 - \frac{m_\ell^2}{t}\right)^2 A_1(t) A_2(t) . \\
& + \frac{m_D^4}{6(m_D + m_{K^*})^2 m_{K^*}^2} \frac{\lambda^{5/2}(m_D^2, m_{K^*}^2, t)}{m_D^{10}} \left(1 + \frac{m_\ell^2}{2t}\right) \left(1 - \frac{m_\ell^2}{t}\right)^2 A_2(t)^2 \\
& \left. + \frac{\lambda^{3/2}(m_D^2, m_{K^*}^2, t)}{m_D^6} \frac{m_\ell^2}{t} \left(1 - \frac{m_\ell^2}{t}\right)^2 A_0(t)^2 \right], \tag{A15}
\end{aligned}$$

where $t = q^2$. The $A_0(t)$ contribution, being proportional to m_ℓ^2 , cannot be measured at current experimental sensitivities. For the other form-factors, the following expressions motivated by vector-meson-dominance [39] is assumed:

$$V(t) = V(0) \frac{1}{1 - t/m_V^2}, \quad A_i(t) = A_i(0) \frac{1}{1 - t/m_A^2}, \quad (i = 1, 2, 3). \tag{A16}$$

The pole masses are taken to be $m_V = m(D_s^{*\pm}) = 2.1 \text{ GeV}$ and $m_A = m(D_{s1}(2460)^\pm) = 2.5 \text{ GeV}$, which are the masses of the lowest lying D_s -mesons with $J^P = 1^-$ and 1^+ , respectively. Experimental data is then fit with the ratios $r_v \equiv V(0)/A_1(0)$, and $r_2 \equiv A_2(0)/A_1(0)$. These ratios have been measured by various experiments via the decay sequence $D^+ \rightarrow \bar{K}^*(892)^0 \ell^+ \nu_\ell$, $\bar{K}^*(892)^0 \rightarrow K^- \pi^+$, most recently by FOCUS [26], which also measured the decay sequence $D^0 \rightarrow K^*(892)^- \mu^+ \nu_\mu$, $K^*(892)^- \rightarrow \bar{K}^0 \pi^-$ [27]. The current world averages are [1]

$$\begin{aligned}
r_v &= \frac{V(0)}{A_1(0)} = 1.62 \pm 0.08, \\
r_2 &= \frac{A_2(0)}{A_1(0)} = 0.83 \pm 0.05. \tag{A17}
\end{aligned}$$

For our purpose, we also need to specify $A_0(t)$ which we assume is of the form

$$A_0(t) = A_3(0) + c_S \frac{t/m_S^2}{1 - t/m_S^2}, \tag{A18}$$

with $m_S = m_{D_s^\pm} = 2.0 \text{ GeV}$, the mass of the lowest lying D_s -meson with $J^P = 0^-$. Normalizing to $A_1(0)$, we have

$$\frac{A_0(t)}{A_1(0)} = r_3 + r_0 \frac{t/m_S^2}{1 - t/m_S^2}, \tag{A19}$$

with

$$r_3 = \frac{(m_D + m_{K^*})}{2m_{K^*}} - \frac{(m_D - m_{K^*})}{2m_{K^*}} r_2 = 1.09 \pm 0.03. \tag{A20}$$

For r_0 , we arbitrarily assume that its 1σ range is $r_0 = 0 \pm r_3$. Substituting Eqs. (A16) and (A19) into Eq. (A15), we obtain the values shown in Fig. 12 for the ratio $(R_{D^+}^*)^{-1} = \Gamma(D \rightarrow K^* e \nu) / \Gamma(D \rightarrow K^* \mu \nu)$. Reading off from the graph, we assign the following 1σ and 2σ ranges:

$$(R_{D^+}^*)^{-1} = 1.060_{-0.003}^{+0.002} (1\sigma), \quad 1.060_{-0.007}^{+0.005} (2\sigma). \tag{A21}$$

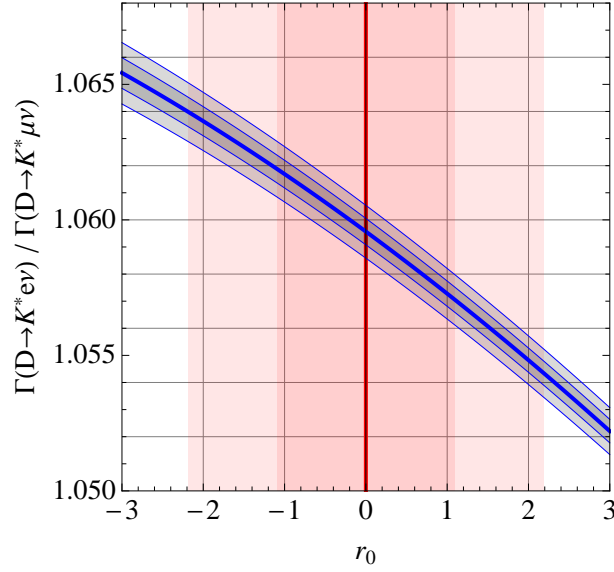


FIG. 12: The dependence of $(R_{D^+}^*)^{-1} = \Gamma(D \rightarrow K^* e \nu) / \Gamma(D \rightarrow K^* \mu \nu)$ on the choice of r_0 . The wide vertical bands are our assumed one- and two-sigma regions of r_0 . The narrow curved bands indicate the one and two-sigma uncertainties due to the error in r_2 . The uncertainty due to errors in r_v , m_D , and m_{K^*} are negligible.

-
- [1] C. Amsler *et al.* [Particle Data Group], “Review of Particle Physics,” Phys. Lett. B **667**, 1 (2008).
[2] S. G. Porsev, K. Beloy and A. Derevianko, Phys. Rev. Lett. **102**, 181601 (2009) [arXiv:0902.0335 [hep-ph]].
[3] S. Banerjee [Babar Collaboration], talk at the 34th International Conference on High Energy Physics, Philadelphia, 29 July-5 August, 2008.
[4] G. Bhattacharyya, Nucl. Phys. Proc. Suppl. **52A**, 83 (1997) [arXiv:hep-ph/9608415];
G. Bhattacharyya, arXiv:hep-ph/9709395;
S. P. Martin, arXiv:hep-ph/9709356;
H. K. Dreiner, arXiv:hep-ph/9707435.
[5] R. Barbier *et al.*, Phys. Rept. **420**, 1 (2005) [arXiv:hep-ph/0406039].
[6] K. S. Babu and R. N. Mohapatra, Phys. Rev. Lett. **75**, 2276 (1995) [arXiv:hep-ph/9506354];
M. Hirsch, H. V. Klapdor-Kleingrothaus and S. G. Kovalenko, Phys. Rev. D **53**, 1329 (1996) [arXiv:hep-ph/9502385];
A. Faessler, S. Kovalenko, F. Simkovic and J. Schwieger, Phys. Rev. Lett. **78**, 183 (1997) [arXiv:hep-ph/9612357];
A. Faessler, S. Kovalenko and F. Simkovic, Phys. Rev. D **58**, 115004 (1998) [arXiv:hep-ph/9803253].
[7] K. Huitu, J. Maalampi, M. Raidal and A. Santamaria, Phys. Lett. B **430**, 355 (1998) [arXiv:hep-ph/9712249].
[8] G. Bhattacharyya and A. Raychaudhuri, Phys. Rev. D **57**, R3837 (1998) [arXiv:hep-ph/9712245].
[9] S. Baek and Y. G. Kim, Phys. Rev. D **60**, 077701 (1999) [arXiv:hep-ph/9906385].
[10] O. Lebedev, W. Loinaz and T. Takeuchi, Phys. Rev. D **61**, 115005 (2000) [arXiv:hep-ph/9910435];
O. Lebedev, W. Loinaz and T. Takeuchi, Phys. Rev. D **62**, 015003 (2000) [arXiv:hep-ph/9911479].
[11] J. P. Saha and A. Kundu, Phys. Rev. D **66**, 054021 (2002) [arXiv:hep-ph/0205046].
[12] S. Bar-Shalom, G. Eilam and Y. D. Yang, Phys. Rev. D **67**, 014007 (2003) [arXiv:hep-ph/0201244].
[13] B. C. Allanach, A. Dedes and H. K. Dreiner, Phys. Rev. D **60**, 075014 (1999) [arXiv:hep-ph/9906209];
B. C. Allanach, A. Dedes and H. K. Dreiner, Phys. Rev. D **69**, 115002 (2004) [Erratum-ibid. D **72**, 079902 (2005)] [arXiv:hep-ph/0309196].
[14] H. K. Dreiner, G. Polesello and M. Thormeier, Phys. Rev. D **65**, 115006 (2002) [arXiv:hep-ph/0112228];
H. K. Dreiner, M. Kramer and B. O’Leary, Phys. Rev. D **75**, 114016 (2007) [arXiv:hep-ph/0612278].
[15] A. Kundu and S. Nandi, Phys. Rev. D **78**, 015009 (2008) [arXiv:0803.1898 [hep-ph]];
P. Dey, A. Kundu, B. Mukhopadhyaya and S. Nandi, JHEP **0812**, 100 (2008) [arXiv:0808.1523 [hep-ph]].
[16] Y. Kao and T. Takeuchi, arXiv:0909.0042 [hep-ph].
[17] D. Chang and W. Y. Keung, Phys. Lett. B **389**, 294 (1996) [arXiv:hep-ph/9608313];
K. Choi, K. Hwang and J. S. Lee, Phys. Lett. B **428**, 129 (1998) [arXiv:hep-ph/9802323];
G. Bhattacharyya and P. B. Pal, Phys. Lett. B **439**, 81 (1998) [arXiv:hep-ph/9806214].
[18] I. Hinchliffe and T. Kaeding, Phys. Rev. D **47**, 279 (1993);
C. E. Carlson, P. Roy and M. Sher, Phys. Lett. B **357**, 99 (1995) [arXiv:hep-ph/9506328];
A. Y. Smirnov and F. Vissani, Phys. Lett. B **380**, 317 (1996) [arXiv:hep-ph/9601387];

- G. Bhattacharyya and P. B. Pal, Phys. Rev. D **59**, 097701 (1999) [arXiv:hep-ph/9809493].
- [19] T. Kinoshita and A. Sirlin, Phys. Rev. **113**, 1652 (1959);
 A. Sirlin, Rev. Mod. Phys. **50**, 573 (1978) [Erratum-ibid. **50**, 905 (1978)];
 T. van Ritbergen and R. G. Stuart, Phys. Rev. Lett. **82**, 488 (1999) [hep-ph/9808283].
- [20] W. J. Marciano and A. Sirlin, Phys. Rev. Lett. **61**, 1815 (1988).
- [21] R. Decker and M. Finkemeier, Nucl. Phys. B **438**, 17 (1995) [hep-ph/9403385].
- [22] A. Ceccucci, Z. Ligeti and Y. Sakai, in Ref. [1].
- [23] R. Kowalewski and T. Mannel, in Ref. [1].
- [24] M. Wirbel, B. Stech and M. Bauer, Z. Phys. C **29**, 637 (1985);
 M. Bauer and M. Wirbel, Z. Phys. C **42**, 671 (1989);
 J. D. Richman and P. R. Burchat, Rev. Mod. Phys. **67**, 893 (1995) [arXiv:hep-ph/9508250].
- [25] J. M. Link *et al.* [FOCUS Collaboration], Phys. Lett. B **607**, 233 (2005) [arXiv:hep-ex/0410037].
- [26] J. M. Link *et al.* [FOCUS Collaboration], Phys. Lett. B **544**, 89 (2002) [arXiv:hep-ex/0207049].
- [27] J. M. Link *et al.* [FOCUS Collaboration], Phys. Lett. B **607**, 67 (2005) [arXiv:hep-ex/0410067].
- [28] L. Widhalm *et al.* [Belle Collaboration], Phys. Rev. Lett. **97**, 061804 (2006) [arXiv:hep-ex/0604049].
- [29] B. Aubert *et al.* [BABAR Collaboration], Phys. Rev. D **76**, 052005 (2007) [arXiv:0704.0020 [hep-ex]].
- [30] S. Dobbs *et al.* [CLEO Collaboration], Phys. Rev. D **77**, 112005 (2008) [arXiv:0712.1020 [hep-ex]].
- [31] D. Besson *et al.* [CLEO Collaboration], Phys. Rev. D **80**, 032005 (2009) [arXiv:0906.2983 [hep-ex]].
- [32] S. Schael *et al.* [ALEPH Collaboration], Phys. Rept. **421**, 191 (2005) [arXiv:hep-ex/0506072].
- [33] M. Artuso *et al.* [CLEO Collaboration], Phys. Rev. Lett. **99**, 071802 (2007) [arXiv:0704.0629 [hep-ex]].
- [34] T. K. Pedlar *et al.* [CLEO Collaboration], Phys. Rev. D **76**, 072002 (2007) [arXiv:0704.0437 [hep-ex]].
- [35] K. M. Ecklund *et al.* [CLEO Collaboration], Phys. Rev. Lett. **100**, 161801 (2008) [arXiv:0712.1175 [hep-ex]].
- [36] L. Widhalm *et al.* [Belle Collaboration], Phys. Rev. Lett. **100**, 241801 (2008) [arXiv:0709.1340 [hep-ex]].
- [37] C. Malbrunot [PIENU Collaboration], talk at Flavor Physics and CP Violation 2009, Lake Placid, NY, May 27-June 1, 2009. See also <https://pienu.triumf.ca/>.
- [38] D. Pocanic *et al.* [PEN Collaboration], arXiv:0909.4358 [hep-ex].
- [39] J. J. Sakurai, Phys. Rev. Lett. **22**, 981 (1969).
- [40] M. Finkemeier and E. Mirkes, Z. Phys. C **72**, 619 (1996) [arXiv:hep-ph/9601275].
- [41] Y. Kao and T. Takeuchi, in preparation.